Title
A SPECTROMETER FOCAL PLANE DETECTOR FOR HEAVY IONS

Author
Harvey, B.G.

Publication Date
1972-04-01

Submitted to Nuclear
Instruments and Methods

LBL-651
Preprint

A SPECTROMETER FOCAL PLANE DETECTOR FOR HEAVY IONS

B. G. Harvey, J. Mahoney, F. G. Pühlhofer, F. S. Goulding,
D. A. Landis, J. C. Faivre, D. G. Kovar, M. S. Zisman,
J. R. Meriwether, S. W. Cosper, and D. L. Hendrie

April 1972

AEC Contract No. W-7405-eng-48

DISCLAIMER

A SPECTROMETER FOCAL PLANE DETECTOR FOR HEAVY IONS*

B. G. Harvey, J. Mahoney, F. G. Pühlhofer†, F. S. Goulding, D. A. Landis, J.-C. Faivre††, D. G. Kovar, M. S. Zisman, J. R. Meriwether‡, S. W. Cosper‡, and D. L. Hendrie

Lawrence Berkeley Laboratory
University of California
Berkeley, California 94720

April 1972

Abstract

A resistive-wire position-sensitive proportional transmission counter has been built for the detection of heavy ions in the focal plane of a magnetic spectrometer. The 45 × 6 cm counter measures position and energy loss with a resolution of 0.7 mm and 8-10% respectively. Time-of-flight is measured with a plastic scintillator behind the proportional counter. The position, time and energy loss signals are used to identify heavy ions with unit mass and atomic number resolution up to about A=20, Z=10.

---

*Work performed under the auspices of the U. S. Atomic Energy Commission.

†Permanent address: Physikaliches Institut, Universität Marburg, Germany.

††Permanent address: CEN Saclay, France.

‡Permanent address: Physics Department, University of Southwestern Louisiana, Lafayette, Louisiana.

1. Introduction

The study of transfer reactions with heavy ions requires a detecting system capable both of high energy resolution and good particle identification. The usual ΔE-E semiconductor telescopes perform less well than with light particles - resolutions of 250-300 keV for heavy ions of 30-60 MeV are typical[1]). Furthermore, separation of ions of the same atomic number Z but different mass number A can be obtained only with ΔE counters of such thickness that they seriously limit the lowest detectable particle energy[2]).

Magnetic spectrometers are free from these difficulties provided that the detector in the focal plane is capable of adequate position resolution and particle identification. Moreover, the large kinematic effects in heavy ion reactions can be compensated by adjustment of the position of the detector[3]). Thus large solid angles may be used without loss of resolution. Finally, energy dispersed rather than energy analyzed beams can be used. This feature is particularly valuable in experiments at cyclotrons and linear accelerators, whose external beams are usually far from monoenergetic, and where the loss of intensity resulting from energy analysis would be very serious.

Since heavy ions are only fully stripped of atomic electrons at the highest energies, four parameters for each ion must be determined. They are A and Z, the mass and atomic numbers, q, the charge state of the ion in flight through the spectrometer magnet, and of course the kinetic energy T. The focal plane position of a particle measures very accurately its magnetic rigidity Bρ from which T can be obtained provided that A and q have been determined.

To measure the four parameters for each particle requires, in the most general situation, the determination of Bρ, velocity (time-of-flight), kinetic

energy and energy loss dE/dx. Measurement of the last quantity is essential because it is the only one of the four whose value (at least for heavy ions of the usual energies) depends on Z. In a detector of the area normally required in a spectrometer focal plane, sufficiently accurate measurement of the kinetic energy is not feasible. Fortunately, measurement of the three quantities $B\rho$, velocity v, and dE/dx, suffices to separate the energy spectra of different particles in most heavy ion nuclear reactions.

Some ambiguities remain in principle. For example, the interaction of ^{16}O ions with a target nucleus could produce overlapping energy spectra of ^{16}O and ^{14}O ions. Measurement of velocity and $B\rho$ can, as described below, separate ions with different values of A/q, but will not separate $^{16}O(8+)$ ions from $^{14}O(7+)$ ions. Measurement of Z will not separate ^{16}O from ^{14}O. The Q-value for the reaction $X(^{16}O,^{16}O')X'$ will nearly always be less negative than $X(^{16}O,^{14}O)Y$, so that at least the high energy end of the ^{16}O spectrum will be free from ^{14}O contamination. Its low energy end, however, may contain $^{14}O(7+)$ ions. Measurements of the $^{14}O(8+)$ spectrum and the intensity ratio of (8+) to (7+) ions might permit subtraction of the $^{14}O(7+)$ contribution to the low energy end of the $^{16}O(8+)$ spectrum.

The focal plane detector to be described measures position (i.e. magnetic rigidity $B\rho$), dE/dx and time-of-flight (velocity) with sufficient precision to permit unit mass and charge resolution for ions up to A=20 and Z=10. In addition, the position resolution (0.7 mm) is compatible with a spectrometer whose energy dispersion is 0.05% per mm.

2. Experimental

2.1. THE PROPORTIONAL COUNTER

The spectrometer[4]) at the Berkeley 88-inch cyclotron was designed for a live focal plane detector: the particle trajectories are very nearly normal to the focal plane. The dispersion -- 3.75 m for dp/p = 1 (p = particle momentum) -- corresponds to a position shift of about 1 mm for an energy change $\Delta E/E \approx 0.05\%$. Energy resolution is about 0.03% at 1 msr solid angle of acceptance. Thus the focal plane detector requires at least 0.5 mm position resolution. For heavy ion experiments even a resolution of 1-2 mm is still much better than can be achieved with alternative systems (E-ΔE silicon counters), which perform very poorly for heavily ionizing particles (they typically give $\Delta E/E \approx 0.5\%$). The focal plane length, 60 cm, corresponds to ~ 30% energy range. Thus the focal plane detector should be rather long (30-60 cm), and capable of better than 2 mm spatial resolution. The vertical size of the image in the center of the focal plane is about five times the vertical size of the beam spot on the target but increases by a further factor of two at the ends of the focal plane. Preliminary tests with a Si(Li) position sensitive detector showed that the system should be sensitive over a vertical height of 6 cm.

The detector, shown in figs. 1 and 2, consists of a resistive - wire proportional counter of the Borkowski-Kopp type[5,6]) with six 0.0025 cm diameter carbon-coated quartz fibers[†], resistance ~ 8,000 Ω/mm, midway between the front and rear high voltage electrodes, which are planes of 0.0006 cm aluminized mylar foils spaced 1 cm apart. The six quartz fibers are spaced vertically one

[†]General Electric Co., Valley Forge, Pa.

above the other with a separation of 1 cm. The horizontal sensitive length is 45 cm which corresponds to an energy range in the spectrometer of 24%. The counter gas (93% Ar + 7% methane) is contained by a front window of 0.0012 cm (non-aluminized) mylar and at the rear by a plastic scintillator - lucite light pipe counter which is used to measure the time-of-flight of particles with respect to the cyclotron oscillator.

Tests with a preliminary version of the proportional counter showed that quartz fibers under low mechanical tension will begin a sustained vibration at some critical value of the applied high voltage which may be well below the potential required to give adequate gas multiplication. The fibers were therefore attached in the manner shown in fig. 3. One end of the fiber was glued with Epoxy resin to a polystyrene insulator button on top of a 0.0075 cm diameter phosphor-bronze wire. The plastic bridge at each end of the counter serves to position the fibers exactly midway between the plane electrodes and exactly 1 cm apart. A spring balance was used to hold the fibers at a tension of 12 g while they were glued to the second polystyrene button mounted on a stiff stainless steel pin. Bending of the phosphor bronze wires (about 2 mm) serves to maintain the fiber tension at a nearly constant value independent of small dimensional changes of the support structure. Electrical contacts to the fiber were made by attaching fine wires to the polystyrene buttons with conducting silver paint. With this arrangement, the counter would support 800 volts when filled with Ar + CH_4 at a pressure of 0.2 atmospheres. Adequate signal to noise ratios were obtained at operating voltages as low as 520 volts. Assuming that the secondary electrons from the window make a negligible contribution to the collected charge, the gas

multiplication is very approximately 2000 at 780 v bias and 0.2 atmospheres pressure. A copper wire embedded in epoxy just below the upper surface of each bridge was connected to a pulse generator. Using the capacitive coupling from the wires to the quartz fibers, artificial pulses from one or both ends can be injected into the fibers to test the electronic system.

To obtain good energy loss information, the aluminized mylar electrodes must be parallel and smooth. Figure 3 shows details of the rear electrode. To improve insulation from the aluminized high voltage surface to the fiber-supporting bridges, the aluminum was removed on both sides of the mylar (with a dilute sodium hydroxide solution) in the vicinity of the bridge. The mylar was stretched as tightly as possible over a large frame, the support surfaces were coated with epoxy resin and the mylar, (still in its frame), was placed in contact with the resin. When the resin had hardened, the mylar was trimmed to its final dimensions and then tensioned by heating it with a jet of hot air. The electrodes thus obtained have the appearance of a good mirror.

The front gas-tight mylar window was glued to its frame. The rounded surface of the frame, against which the mylar is tightly pressed by the internal gas pressure, was lubricated with Teflon aerosol. With no lubrication, slipping of the mylar over the surface as it stretched during inflation took place in a series of jerks accompanied by a creaking noise, and pinhole leaks usually developed. The 0.0012 cm - thick window is operated at a maximum pressure of 0.4 atmospheres. Its breaking pressure is $\sim$ 0.6 atmospheres.

Good dE/dx resolution requires that the pressure and purity of the counter gas remain constant. These requirements are met by a continuous gas flow system at a pressure regulated by a Nullmatic Model 44-20 regulator[†].

[†]Moore Products, Spring House, Pa.

2.2. THE SCINTILLATION COUNTER

The time-of-flight detector consists of a Pilot-F plastic scintillator 0.316 cm thick glued to a Lucite light pipe to the end of which was glued an RCA 8575 photomultiplier. Signals are taken from the 9th dynode (for pulse height information) and from the anode (for fast timing).

2.3. ELECTRONICS

Position of a particle is measured by the rise-time comparison method described by Borkowski and Kopp[5]).

Figure 4 shows the circuit of one of the twelve voltage-sensitive preamplifiers: Figure 5 shows a block diagram of the electronics.

Signals from each preamplifier are examined for pulse height with respect to an adjustable threshold voltage. Signals larger than the threshold generate a logic signal to denote which fiber detected the particle so that the six position spectra can be stored separately. An additional logic signal denotes that two fibers detected simultaneous events. All such events are stored in a seventh spectrum in the Nuclear Data analyzer. The threshold is required because a pulse on a wire is accompanied by a small signal on an adjacent wire. Only very rarely does a particle induce signals of comparable size on two wires.

The outputs of the six preamplifiers at each end are mixed and the two mixed outputs are amplified to produce Gaussian-shaped pulses with 8 μs peaking time. Differentiation and cross-over detection produce timing signals which are used (one of them passing through an adjustable delay) to start and stop a time-to-amplitude converter (TAC). The maximum time delay between start and stop pulses is about 20 μs.

Our early work on resistive-wire proportional counters indicated a serious problem in achieving linearity of the output from the TAC as a function of position. The non-linearity was not restricted to points near the end of the wire, but extended out at least 25% of the wire-length at each end. Investigation showed that the non-linearity is affected markedly by the termination of the wire, and also by the type, and time-constant, of the pulse-shaping networks used to produce the biphase signals from which crossover timing pulses are derived. Figure 6 shows the behaviors under two conditions of termination using simple RC differentiation and integration. As shown in this curve, a very low value of terminating capacity causes curvature with the output falling low toward the ends. The reverse situation occurs if the capacity is too high. As shown in fig. 6, the optimum value of capacitor produces a slight S-shaped distortion. By including a resistor in series with the capacitor a practically linear response is achieved. Components R1, C1 in fig. 4 serve this purpose while resistor R2 (100MΩ) serves to provide the dc path to ground for the gate of Q1. The bootstrap arrangement shown in fig. 4 reduces all stray capacity to ground effectively to zero so that C1 is by far the dominant terminating capacity.

Energy-loss signals are obtained by adding the pulses from the ends of all the fibers. Since the preamplifier signal rise times are a function of position, it is necessary to use an amplifier with 16 μs peaking time. Even though the dE/dx system contains the mixed noise of all twelve preamplifiers, the resolution is not limited by the signal-to-noise ratio even at quite small values of the gas multiplication. The total noise is typically 50-100 mv for signals of 6 v.

Time-of-flight modulo the cyclotron period is measured by the scintillation counter, light pipe and RCA 8575 photomultiplier. The photomultiplier anode signal and a signal from the cyclotron oscillator are used to start and stop a TAC. The light output from the Pilot-F scintillator is highly saturated for heavy ions at energies below several hundreds of MeV: it is therefore approximately proportional to the range of the particles. This information would be valuable for particle identification were it not for the poor resolution (12 1/2% for 150 MeV ^{20}Ne ions) and the almost total lack of information about the scintillator response as a function of particle mass, atomic number and velocity. The intrinsic time resolution of the system appears to be better than 2 ns: in practice the resolution is determined entirely by the cyclotron beam pulse width.

Complications introduced by the very different rise times of the position, dE/dx and time-of-flight signals are solved as shown in fig. 5 in a conceptually straight-forward manner. After digitizing in a 4000-channel analogue to digital converter, the signals and fiber-identification pulses are stored both on tape and in an SCC-660 computer (32K memory of 24 bit words plus disc storage of 800 K words). Details of the heavy ion identification method are described below.

3. Results

3.1. POSITION RESOLUTION

Position resolution was measured in the spectrometer with 60 MeV ^{16}O ions elastically scattered from a thin target of ^{197}Au. A 0.5 mm wide slit was placed in front of the proportional counter to separate the measured resolution from all effects arising from reaction kinematics, target

non-uniformity, spectrometer aberrations etc. The TAC output as a function of position was calibrated by changing the spectrometer field so that the elastic peak fell at two points on the counter bracketing the position of the slit. The magnetic field values were measured with an NMR system. If ν_1, ν_2, and ν_c respectively represent the NMR frequencies for the two calibration points and the slit position, the intrinsic energy resolution of the counter in the spectrometer is

$$\Delta E/E = \frac{2(\nu_1 - \nu_2)\Delta V}{\nu_c \bar{V}} \cdot E_{16_0}$$

where ΔV is the measured full width of half maximum of the TAC signal obtained through the slit, $\bar{V}$ is the average of the TAC signals at the calibration points and E_{16_0} is the ^{16}O ion kinetic energy.

$\Delta E/E$ was found to be 28 keV. From the calculated momentum dispersion of the spectrometer, 3.75 m, this value corresponds to a position resolution (FWHM) of 0.88 mm. From this, the rectangular distribution 0.5 mm wide due to the slit must be subtracted, leaving an intrinsic counter resolution of about 0.7 mm. This value still includes a contribution from slit scattering.

3.2. dE/dx RESOLUTION

The resolution in the dE/dx signal appears to be determined largely by the straggling in the energy loss of particles in the counter gas. Calculations of the straggling[7]) are compared with some measured values of the dE/dx resolution in Table 1.

Table 1 shows that the dE/dx resolution for 104 MeV ^{16}O ions improved significantly when the counter gas pressure was doubled. The experimental value is given approximately by:

$$(\text{Expt. resolution})^2 = (\text{Calculated straggling})^2 + 25$$

Figure 7 shows the change of dE/dx pulse height as a function of counter bias at 0.2 and 0.4 atmospheres counter gas pressure. Raising the gas pressure at constant bias produces a roughly proportional decrease in pulse height. To limit changes in dE/dx signal due to pressure fluctuations to 1% therefore requires that the gas density be stable to about 1%.

That the dE/dx signal be independent of position along the counter for ions of a given energy loss is not important. Since the position is always known, a correction can be made. At a constant magnetic field and for an ion of fixed A and Z, dE/dx should be (and indeed is) lower for particles that fall on the right hand (high energy) end of the counter. There is an instrumental effect of unknown origin that nearly compensates for the drop. As will be discussed below, dE/dx is corrected empirically to remove position dependence. Figure 8 shows a dE/dx spectrum obtained after making this correction.

When the counter bias is too high (above about 700 v at 0.4 atmos. pressure), dE/dx peaks from heavy ions begin to develop a "tail" on the high energy side.

3.3. TIME RESOLUTION

The flight path from target to focal surface is about 7 m: flight times for heavy ions are typically 250 ns. There is a small dispersion of about 1 ns in the flight time depending on the angle at which a particle leaves the target. This dispersion can be made arbitrarily small by closing slits between target and spectrometer, but it is too small to present any difficulty.

The flight path is also a function of the position at which a particle intersects the focal surface, but since that position is always known, the time-of-flight can be corrected as discussed below.

In practice the time resolution is determined by the pulse width of the cyclotron beam, which varies as a function of many parameters. Third harmonic acceleration generally gives better resolution, but of course cannot be used for higher energy beams. Figure 9 shows the measured time distribution obtained by scattering 60 MeV ^{16}O ions from ^{197}Au: the acceleration was on third harmonic. A time spectrum of scattered particles that were accelerated on the first harmonic is shown in fig. 10.

Satellite time peaks are frequently observed but can be reduced to acceptable intensities by adjustment of the cyclotron frequency, dee voltage or harmonic coils with little loss of beam intensity. The resultant time resolution is typically 4-7 ns.

4. Particle Identification

The signals on each wire corresponding to position, energy loss, time-of-flight and scintillator pulse height are digitized in a 4096-channel ADC-multiplexer and stored in the SCC-660 computer. Upon arrival of each 48 events, the information is written on magnetic tape.

The computer permits oscilloscope display of all the singles spectra as well as displays of time-of-flight vs. position, dE/dx vs. position, scintillator dynode signal vs. position and time-of-flight vs. dE/dx. The measured quantities are related to the particle parameters in the following way (for non-relativistic heavy particles):

$$\text{Position} = X \propto B\rho \propto Av/q$$

$$dE/dx \propto z^2(A/E)^{1/2} \propto Z^2/v$$

A display of time-of-flight (1/v) vs. position therefore consists of curves each of which corresponds to a unique value of A/q. In practice, only time differences ΔT are measured.

To obtain a signal independent of a particle's position, a correction is applied to the measured time-of-flight ΔT:

$$TOF(corr) = (T_0 + \Delta T)\ (1 + \alpha X)$$

where T_0 and α are empirically chosen constants and X is the position of a particle along the counter. A typical display of TOF (corr) vs. X is shown in fig. 11. Windows can be set to select chosen values of A/q.

The dE/dx signal is corrected for its position dependence by:

$$(dE/dx)_{corr} = dE/dx(1 + \beta X)$$

Figure 12 shows a display of $(dE/dx)_{corr}$ vs. X for all values of A/q. Particles of different Z are well-separated by the dE/dx signal. Figure 13 shows a display of corrected time-of-flight vs. corrected dE/dx. Particle types separate into discrete spots according to their values of Z and A/q: this display is particularly useful when adjusting the computer gates on dE/dx and time-of-flight in order to select a chosen particle type. Identification of particle types during the course of an experiment is facilitated by making prior calculations of the TOF vs. X and dE/dx vs. X plots. The calculations

are remarkably close to the experimental results. The computer is capable of processing and storing about 50 events per second. During tape-writing no events are accepted, so a signal from the computer gates off all analyzers, scalers, a clock and the beam integrator. Final reduction of results is done off-line by replaying the data tapes.

Even after adjustment of the preamplifier network, position linearity is not quite perfect, nor are all wires identical. Adding spectra from all six wires therefore produces a total spectrum with an unacceptable loss of resolution. Figure 14 (upper) shows a spectrum obtained by adding the separate spectra from all wires. The spectrum from a single wire is shown in the lower half of the figure. The loss of resolution by simple adding is clearly visible.

For each wire, true position X *vs.* channel number C can be measured by means of a collimated ^{241}Am α-particle source mounted on a lead-screw parallel to the counter. A least-squares fit of this calibration gave the following result:

$$\text{WIRE 1} \quad X = -22.7894 + 0.1142C - 2.2654 \times 10^{-4} C^2 + 1.0087 \times 10^{-6} C^3$$

$$\text{WIRE 2} \quad X = -22.5930 + 0.1048C - 1.5542 \times 10^{-4} C^2 + 6.0649 \times 10^{-7} C^3$$

$$\text{WIRE 3} \quad X = -22.9347 + 0.1124C - 2.9380 \times 10^{-4} C^2 + 1.9523 \times 10^{-6} C^3$$

$$\text{WIRE 4} \quad X = -22.7490 + 0.1093C - 1.1452 \times 10^{-4} C^2 + 2.1509 \times 10^{-7} C^3$$

$$\text{WIRE 5} \quad X = -22.3505 + 0.0078C + 3.3257 \times 10^{-4} C^2 - 3.1713 \times 10^{-6} C^3$$

$$\text{WIRE 6} \quad X = -21.7064 + 0.0080C + 2.0770 \times 10^{-4} C^2 - 2.0235 \times 10^{-6} C^3$$

By means of these six equations, all spectra can be converted to true position spectra and added with little loss of resolution. The top spectrum of

fig. 15 was obtained in this way: it is to be compared with the lower spectrum of fig. 14 (a single wire) and the upper spectrum (all six wire spectra simply added).

The lower spectra of fig. 15 show individual particle types separated out from the upper spectrum. The ^{16}O peak comes from elastic scattering of a small $^{16}O(4+)$ contaminant in the $^{12}C(3+)$ cyclotron beam. The separation of ^{13}C from the enormous ^{12}C elastic peak is especially satisfying.

Energy resolution is typically 0.015%. In some test runs a resolution of 0.01% has been obtained but under the practical conditions of target thickness, beam emittance and spectrometer solid angle that are used in an experiment, the resolution is not quite so good. In any event, the position resolution and stability of the counter do not appear to be a limiting factor.

5. Conclusions

The Borkowski-Kopp proportional counter, when operated with end terminations and shaping as described above, provides a relatively simple method for making simultaneous position and energy-loss measurements. The system described here can undoubtedly be improved. Among the many parameters that have not been systematically investigated to optimize performance are 1) quartz fiber diameter and resistance 2) vertical fiber separation 3) counter depth 4) counter gas pressure and 5) counter gas mixture. The counter can probably be adapted to the detection of light particles by operating it at higher gas pressure and bias. Time resolution can probably be improved to $\sim$ 2 ns (or $\sim$ 1%) by detection of secondary electrons from a very thin foil at the entrance to the spectrometer[8]) to make a time-zero signal. Time resolution would then be independent of cyclotron tuning and it should be possible to

separate adjacent mass values at the same charge up to A = 40-50. Improvement of dE/dx resolution by increasing the energy loss should be possible. Calculations[7]) show that the energy loss straggling for 60 MeV ^{16}O ions becomes only 2% when the energy loss is increased to 10 MeV. A resolution of even 5% in dE/dx, corresponding to 2.5% in Z, would permit separation of adjacent elements up to Z = 20.

Acknowledgements

We wish to thank Roy F. Burton for making the mechanical design, members of the Cyclotron Accelerator Technician Shop for construction of the parts, Stuart D. Wright for building the special electronics, and David J. Clark, Jacques Steyaert, and John Bowen and the cyclotron operating staff for making excellent heavy ion beams.

References

1) J.-C. Faivre, H. Faraggi, J. Gastebois, B. G. Harvey, M.-C. Lemaire, J.-M. Loiseaux, M. C. Mermaz, and A. Papineau, Phys. Rev. Letters 24 (1970) 1188.

2) A. H. Poskanzer, private communication.

3) D. L. Hendrie, in Nuclear Spectroscopy (J. Cerny, ed.), 3rd Edition, Chapter III.C, Academic Press, New York (1972).

4) D. L. Hendrie, J. R. Meriwether, and F. B. Selph, to be published. J. B. Selph, UCID-3388, Lawrence Berkeley Laboratory (1969).

5) C. J. Borkowski and M. K. Kopp, IEEE Transactions on Nucl. Sci. NS 17 No. 3 (1970) 340.

6) J. L. C. Ford, P. H. Stelson, and R. L. Robinson, Nucl. Instr. Methods 98 (1972) 199.

7) C. C. Maples, private communication (1972).

8) W. F. W. Schneider, B. Kohlmeyer, and R. Bock, Nucl. Instr. Methods 87 (1970) 253.

Table 1. Comparison of calculated energy loss straggling and measured dE/dx resolution.

Particle	Energy (MeV)	Gas Pressure (Atmos.)	Energy Loss (MeV)	dE/dx Resolution (%) Calc.(1)	Expt.
^{16}O	60	0.2	1.35(1)	6.8	9.0
^{16}O	104	0.2	0.9(1)	10.2	11.6
^{16}O	104	0.4	1.8(1)	7.1	8.5
^{16}O	140	0.4	1.5(1)	9.2	10.5
^{20}Ne	150	0.4	~ 2.2	—	9.0
^{4}He	25	0.2	~ 0.057(1)	40	~ 30

Note: 1) Calculated, ref. 7.

Figure Captions

Fig. 1. General view of the counter system.

Fig. 2. Detail of one end of the counter. The main frames are fiberglass-epoxy.

Fig. 3. Detail of quartz fiber support.

Fig. 4. Circuit of one preamplifier.

Fig. 5. Block diagram of the electronics.

Fig. 6. Effect of termination on counter position linearity.

Fig. 7. Relative gas multiplication as a function of counter bias at 0.2 and 0.4 atmos. pressure.

Fig. 8. Corrected dE/dx singles spectrum, 150 MeV ^{20}Ne on ^{27}Al.

Fig. 9. Time spectrum obtained by elastic scattering of 60 MeV ^{16}O ions accelerated in third harmonic mode. The right-hand peak was obtained by introducing a 4 ns delay for calibration purposes.

Fig. 10. Time spectrum obtained from reaction products of 104 MeV ^{16}O ions on ^{208}Pb. The left peak is ^{16}O, the center peak is $^{15}N + ^{17}O$. The ^{16}O ions were accelerated in the first harmonic mode. The peak widths are about 5.5 ns.

Fig. 11. Two-dimensional display of corrected time-of-flight vs. position showing bands of constant A/q. Dots are intensified on a logarithmic scale. 104 MeV ^{16}O on ^{208}Pb.

Fig. 12. Two-dimensional display of corrected dE/dx vs. position showing bands of constant Z. Dots are intensified on a logarithmic scale. 78 MeV ^{12}C on ^{54}Fe.

Fig. 13. Two-dimensional display of corrected time-of-flight vs. corrected dE/dx showing separation into spots according to A/q and Z. Ions are identified in the key below. 78 MeV ^{12}C on ^{54}Fe.

Fig. 14. Total position spectrum obtained by adding six separate wire spectra (upper). Spectrum from a single wire (lower).

Fig. 15. The upper spectrum was obtained by merging six wire spectra by the α-source calibration method described in the text. The lower spectra are obtained from the upper by separation of individual particle types.

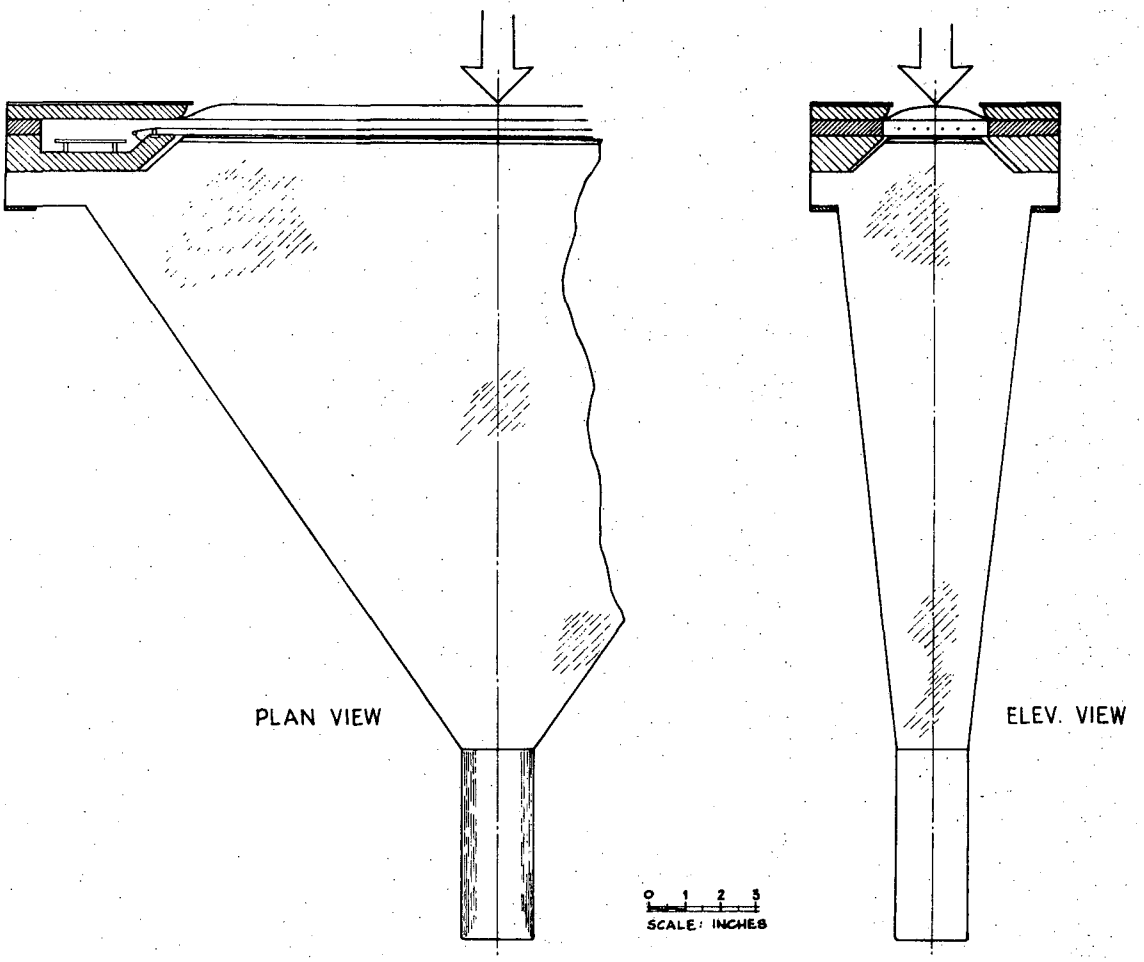

Fig. 1

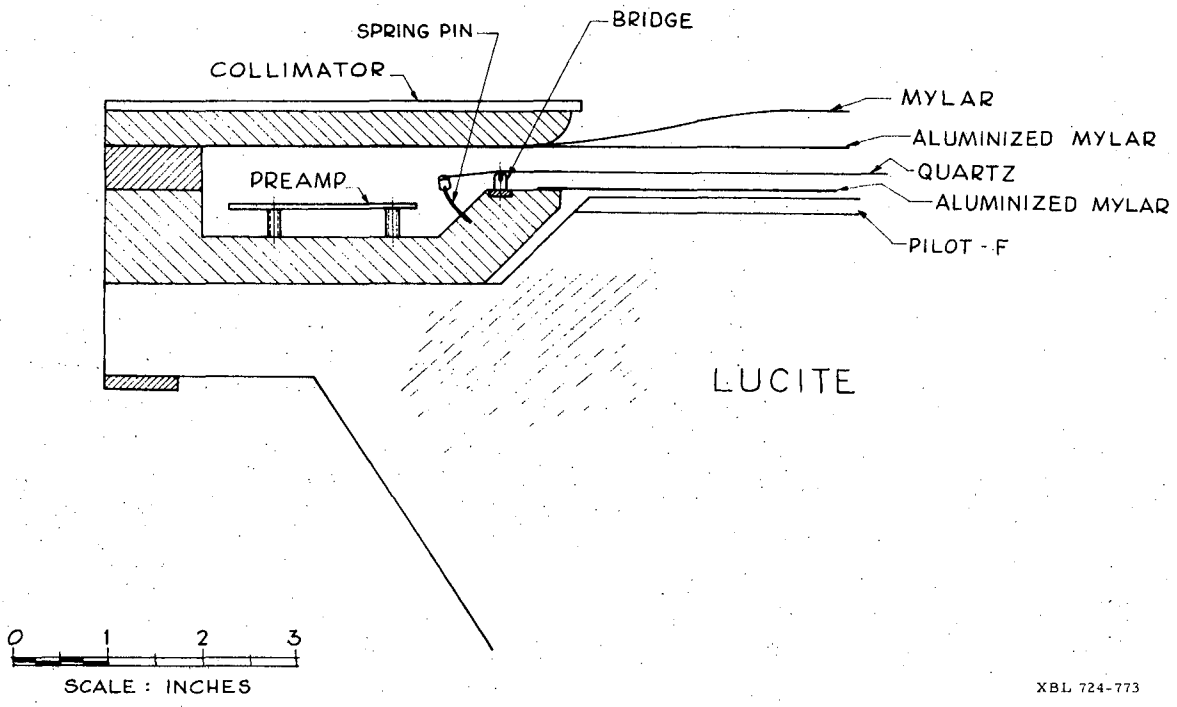
SPRING PIN
BRIDGE
COLLIMATOR
MYLAR
ALUMINIZED MYLAR
QUARTZ
ALUMINIZED MYLAR
PILOT - F
PREAMP
LUCITE
0 1 2 3
SCALE : INCHES
XBL 724-773

Fig. 2

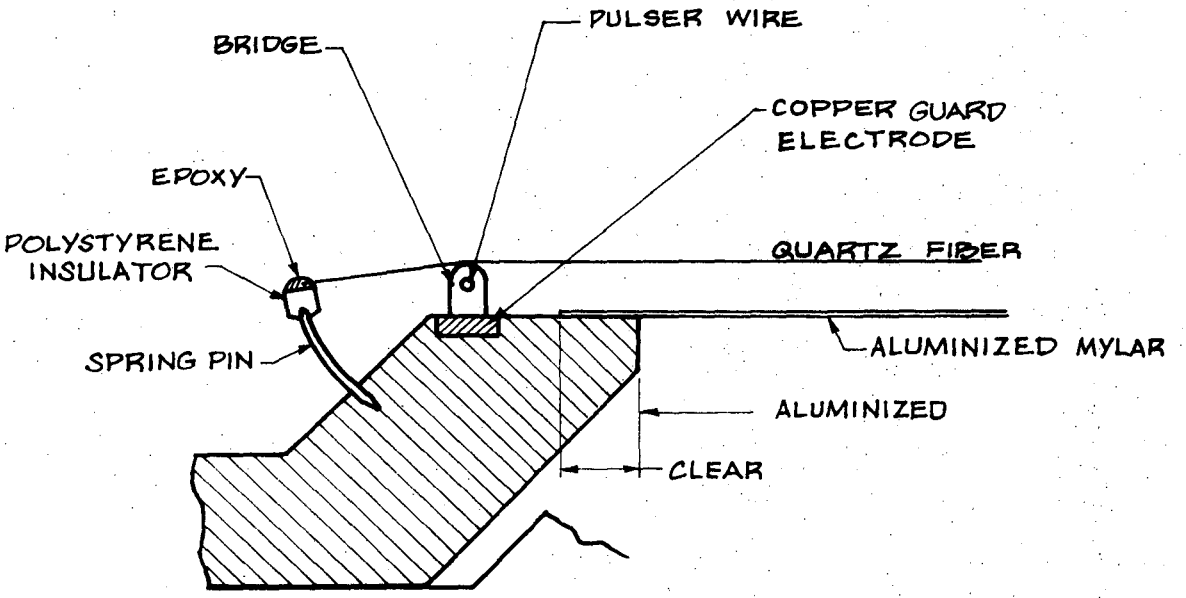

XBL 724-771

Fig. 3

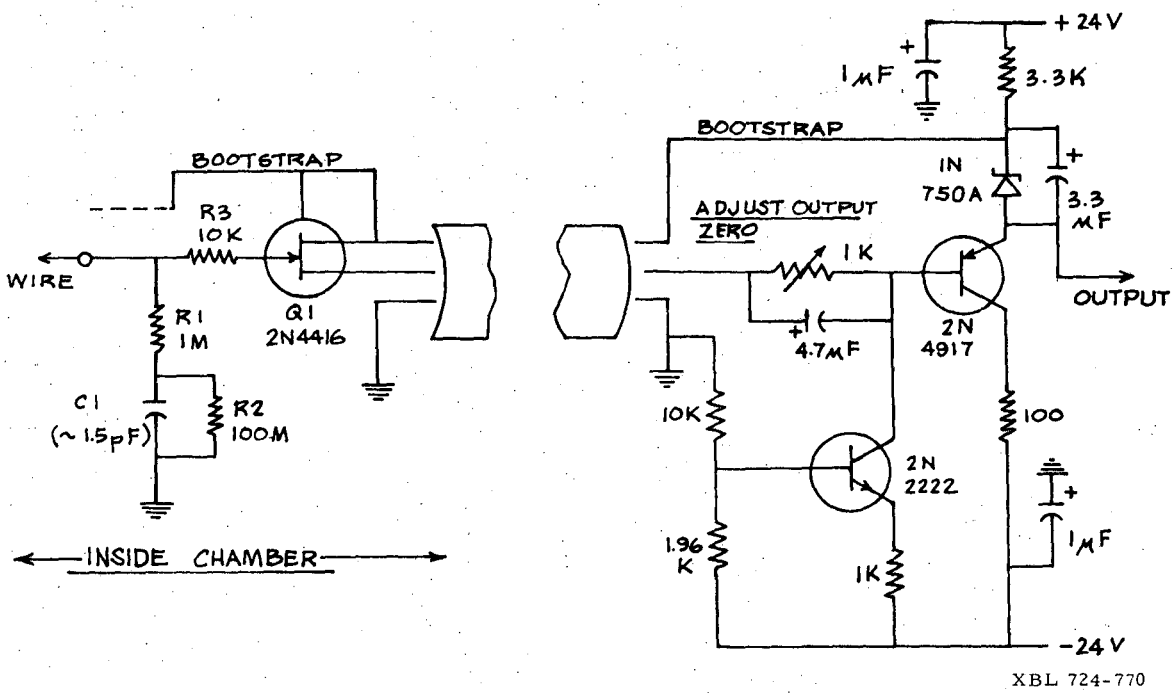
BOOTSTRAP
R3
10K
WIRE
R1
1M
Q1
2N4416
C1
(~1.5pF)
R2
100M
INSIDE CHAMBER
+24V
1μF
3.3K
BOOTSTRAP
IN
750A
3.3
μF
ADJUST OUTPUT
ZERO
1K
OUTPUT
4.7μF
2N
4917
10K
100
2N
2222
1.96
K
1K
1μF
-24V
XBL 724-770

Fig. 4

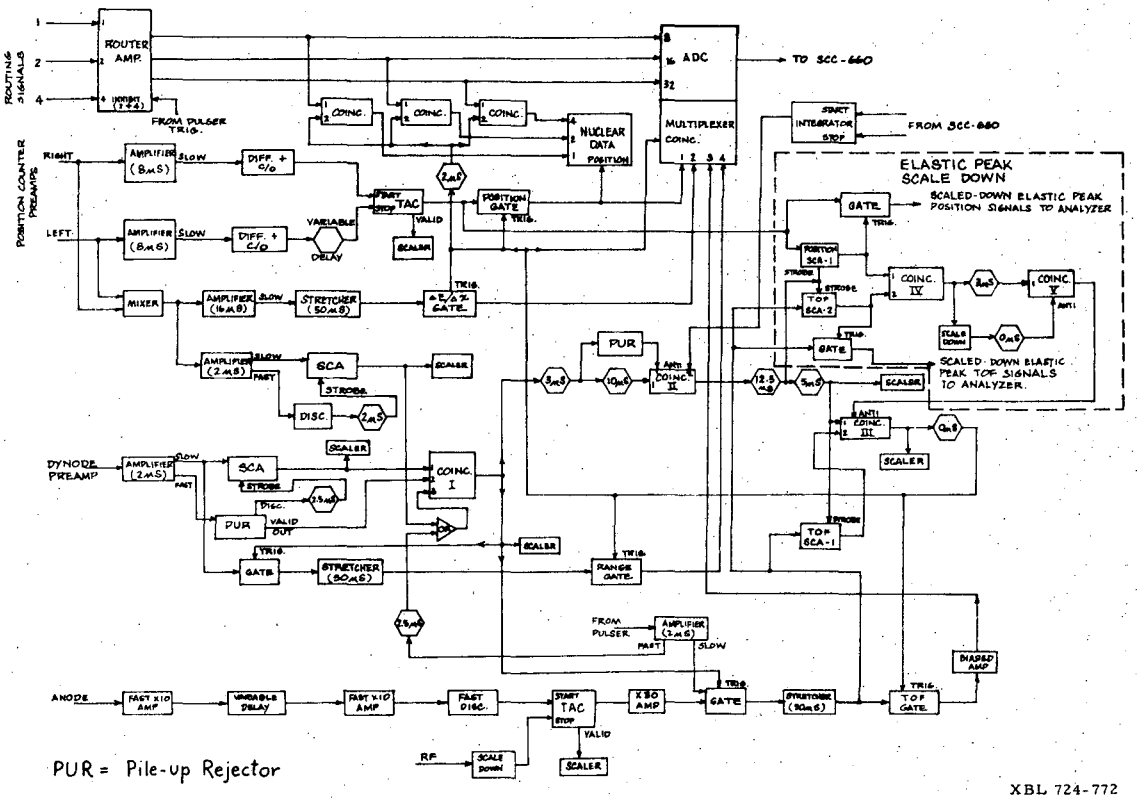
ROUTING SIGNALS
ROUTER AMP.
FROM PULSER TRIG.
ADC
TO SCC-660
MULTIPLEXER
NUCLEAR DATA
POSITION
COINC.
START INTEGRATOR STOP
FROM SCC-660
ELASTIC PEAK SCALE DOWN
SCALED-DOWN ELASTIC PEAK POSITION SIGNALS TO ANALYZER
POSITION COUNTER PREAMPS
RIGHT
LEFT
AMPLIFIER (8mS)
SLOW
DIFF. + C/O
TAC
START
STOP
VALID
SCALER
VARIABLE DELAY
POSITION GATE
MIXER
AMPLIFIER (16mS)
STRETCHER (50mS)
A.E./A.T. GATE
TRIG.
AMPLIFIER (2mS)
FAST
SCA
STROBE
DISC
DYNODE PREAMP
PUR
VALID OUT
GATE
STRETCHER (50mS)
RANGE GATE
FROM PULSER
AMPLIFIER (2mS)
ANODE
FAST x10 AMP
VARIABLE DELAY
FAST x10 AMP
FAST DISC.
START TAC
STOP
VALID
X50 AMP
GATE
STRETCHER (90nS)
TOP GATE
BIASED AMP
RF
SCALE DOWN
SCALER
TOP SCA-1
TOP SCA-2
POSITION SCA-1
COINC. I
COINC. II
COINC. III
COINC. IV
COINC. V
ANTI
SCALE DOWN
SCALED-DOWN ELASTIC PEAK TOF SIGNALS TO ANALYZER.
PUR = Pile-up Rejector
XBL 724-772

Fig. 5

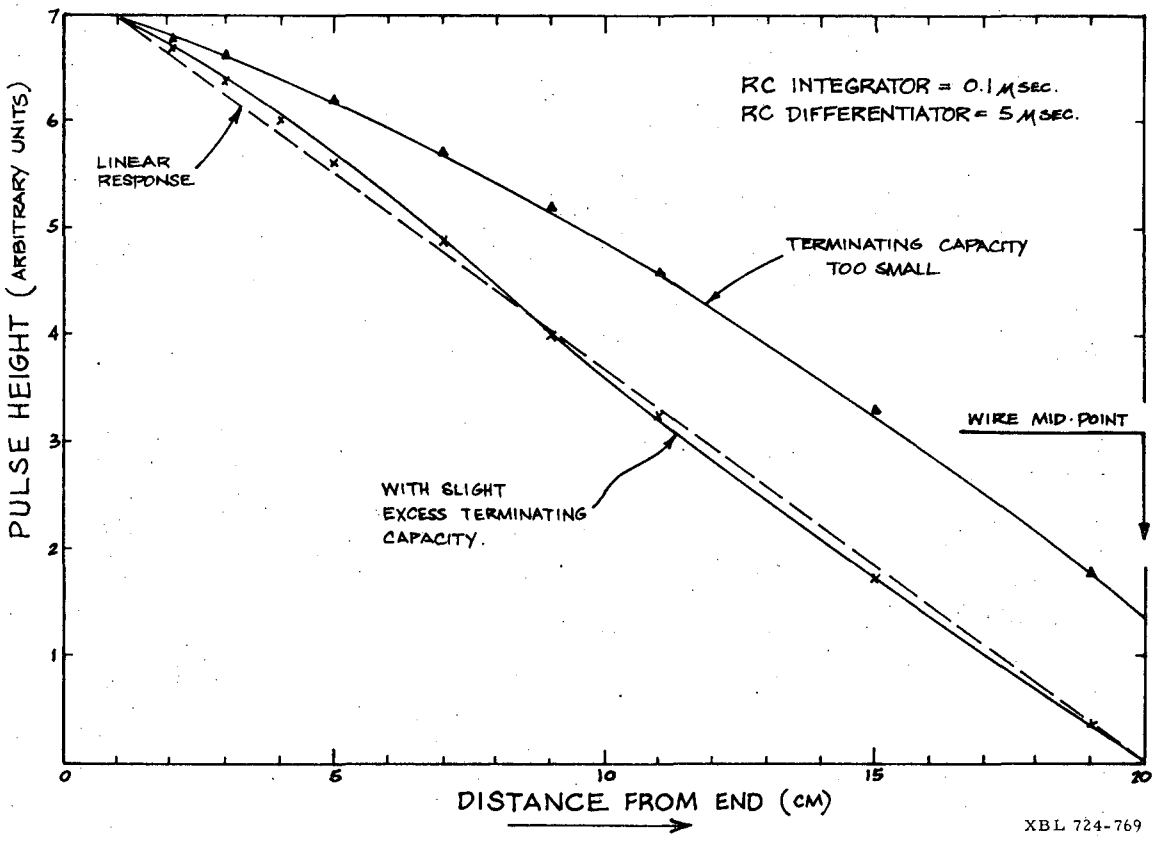
RC INTEGRATOR = 0.1 μsec.
RC DIFFERENTIATOR = 5 μsec.
LINEAR RESPONSE
TERMINATING CAPACITY TOO SMALL
WIRE MID-POINT
WITH SLIGHT EXCESS TERMINATING CAPACITY.
PULSE HEIGHT (ARBITRARY UNITS)
DISTANCE FROM END (cm)
0
5
10
15
20
1
2
3
4
5
6
7
XBL 724-769

Fig. 6

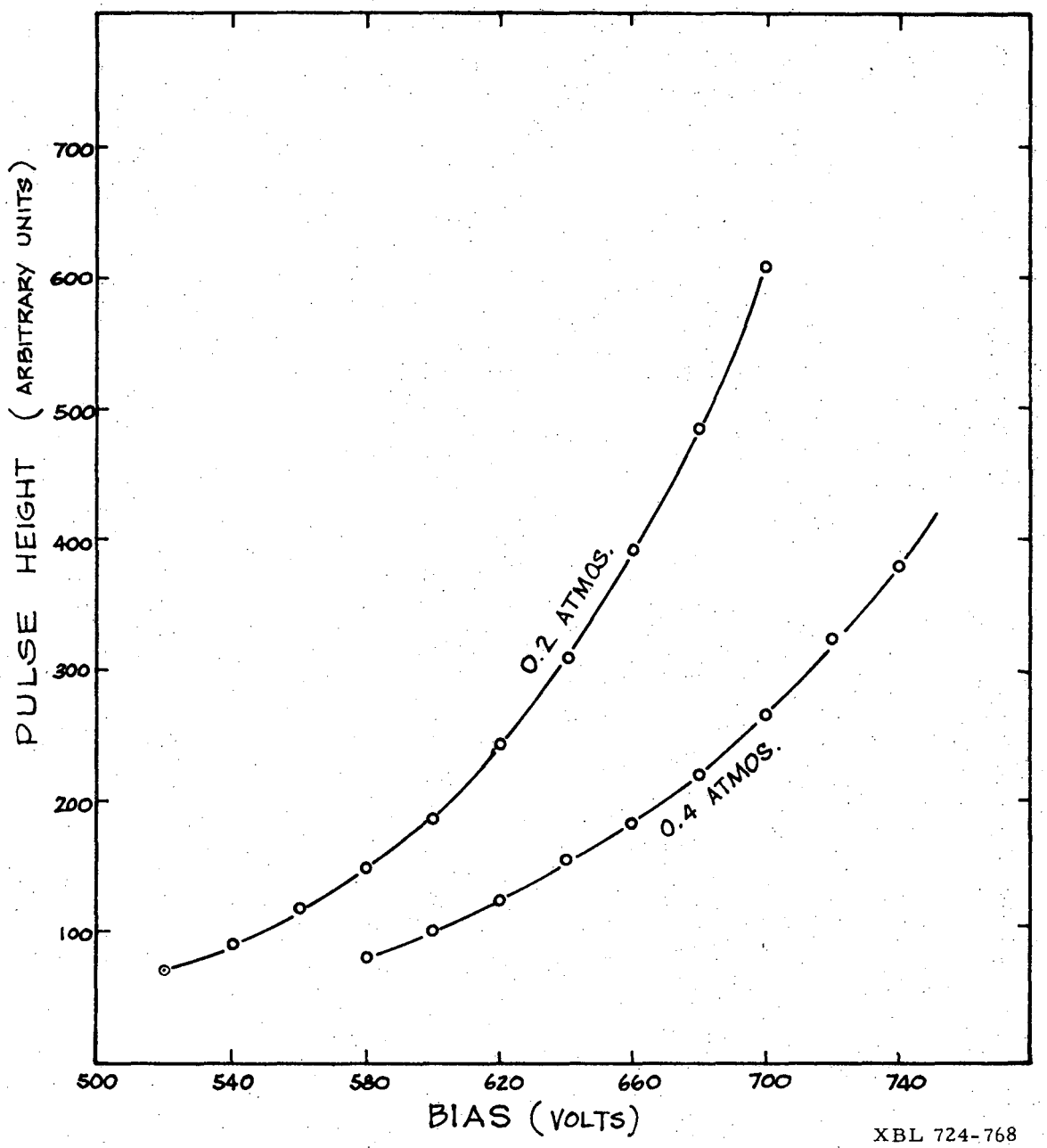
PULSE HEIGHT (ARBITRARY UNITS)
700
600
500
400
300
200
100
0.2 ATMOS.
0.4 ATMOS.
500
540
580
620
660
700
740
BIAS (VOLTS)
XBL 724-768

Fig. 7

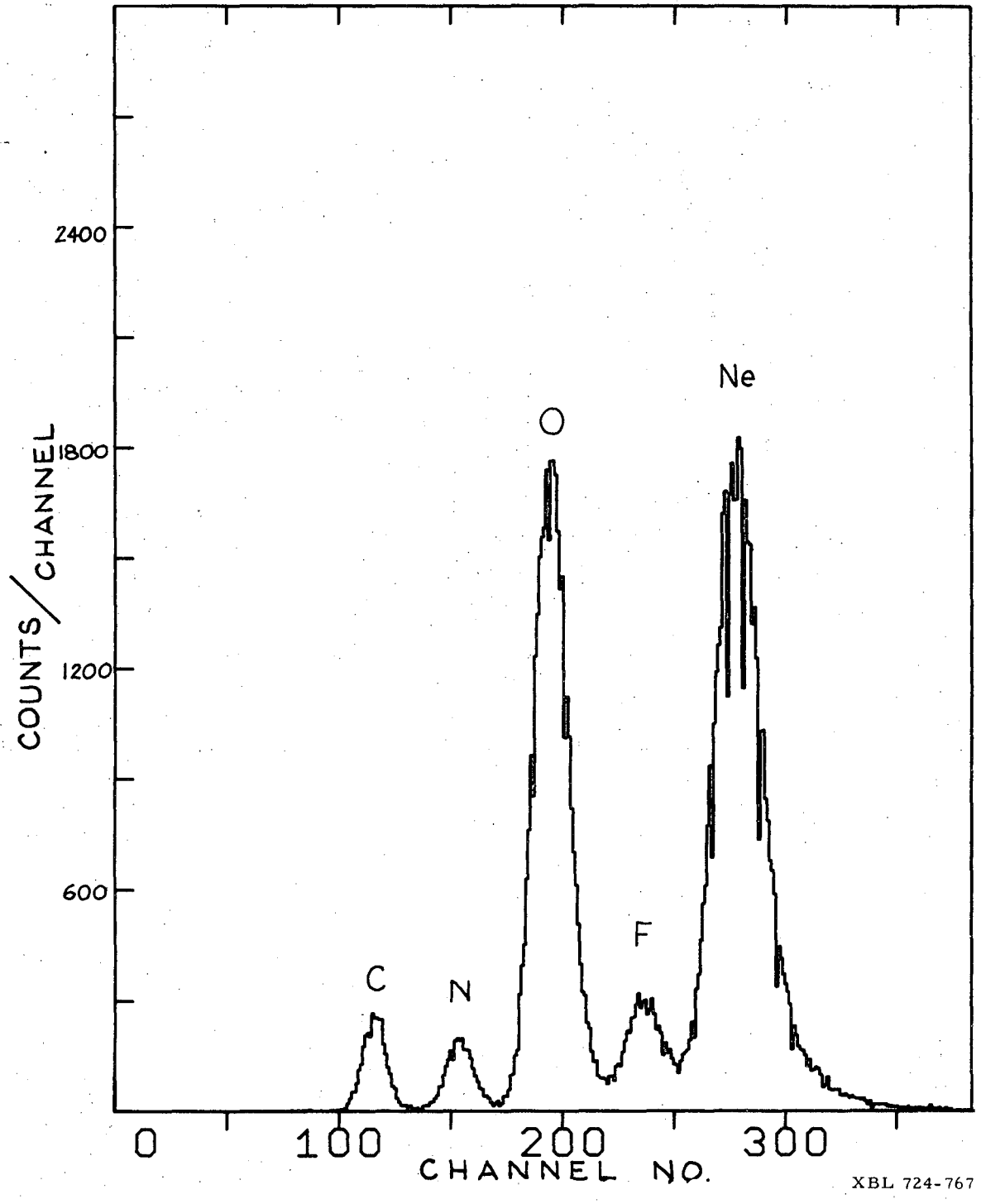
2400
1800
1200
600
COUNTS/CHANNEL
C
N
O
F
Ne
0
100
200
300
CHANNEL NO.
XBL 724-767

Fig. 8

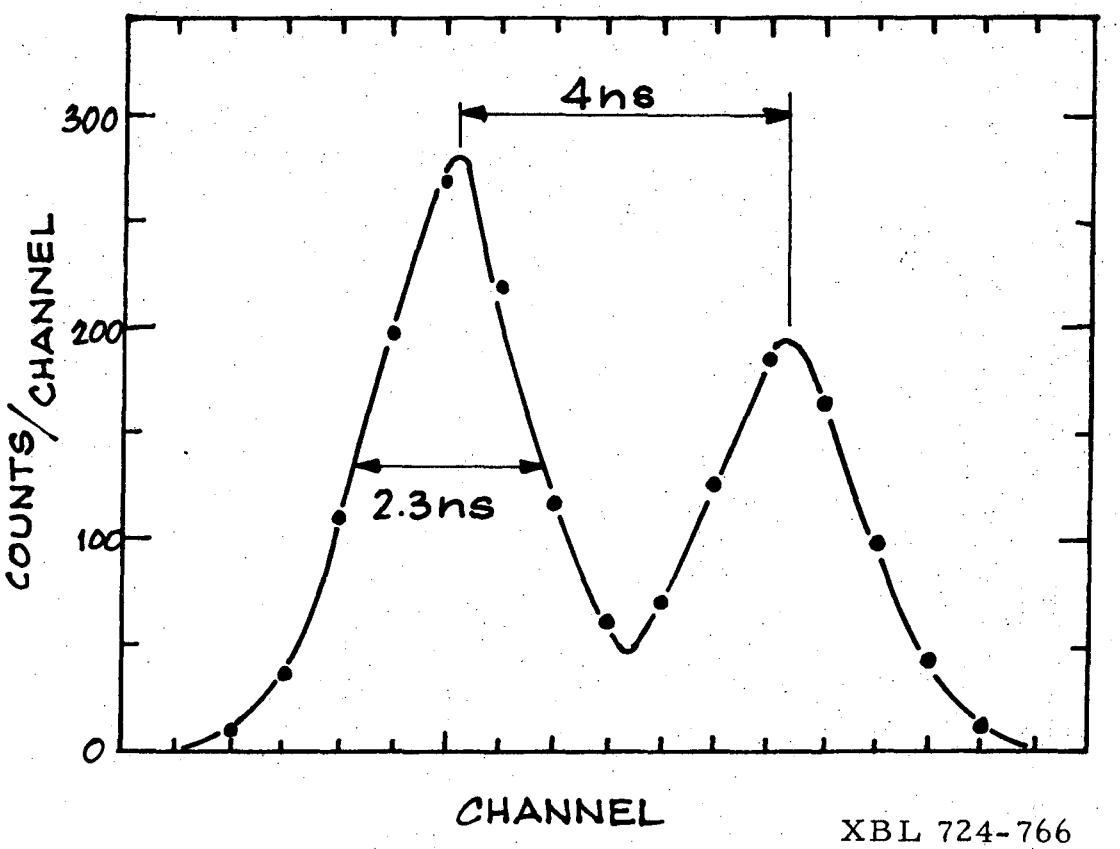

Fig. 9

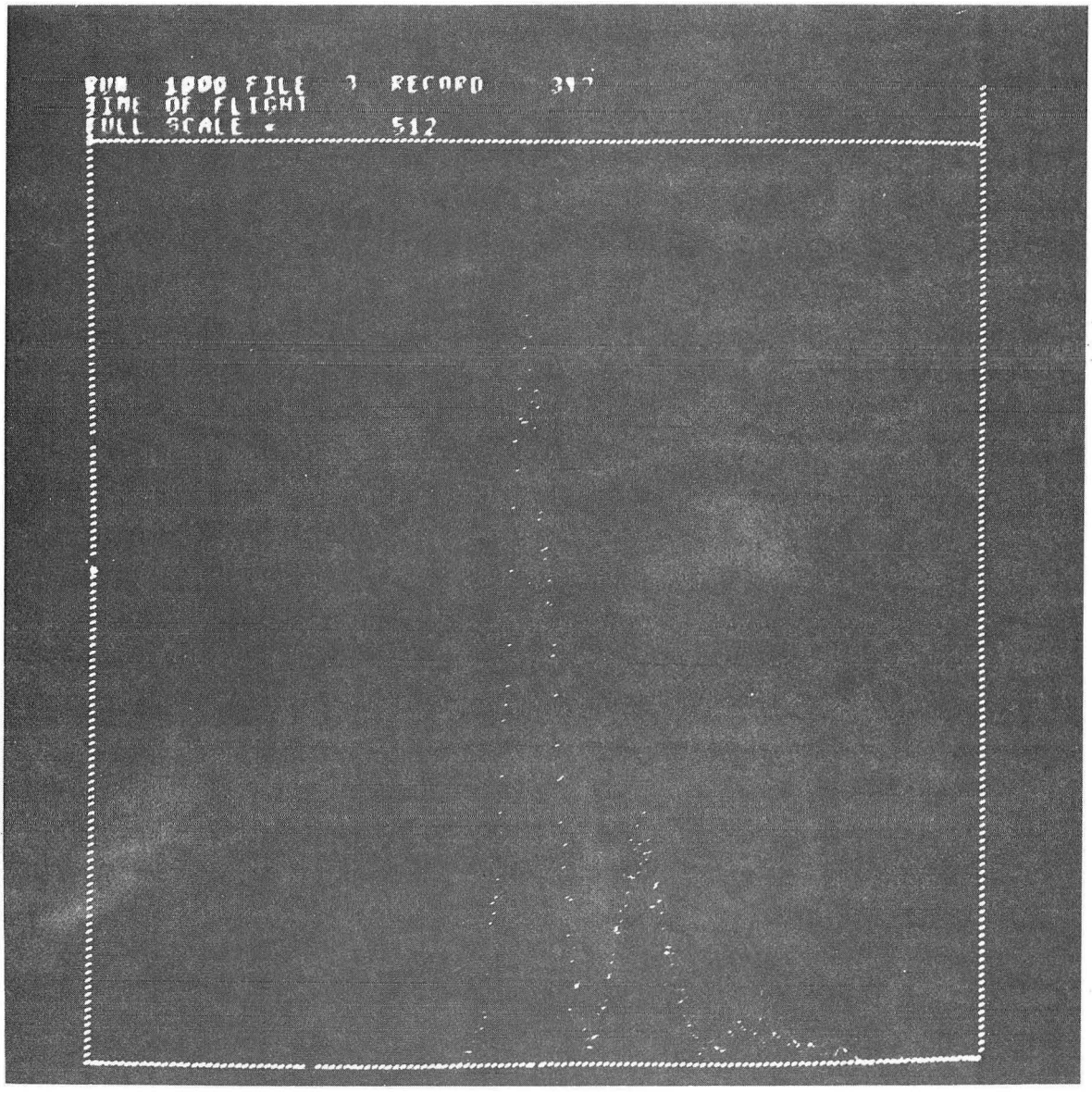

XBB 721-421

Fig. 10

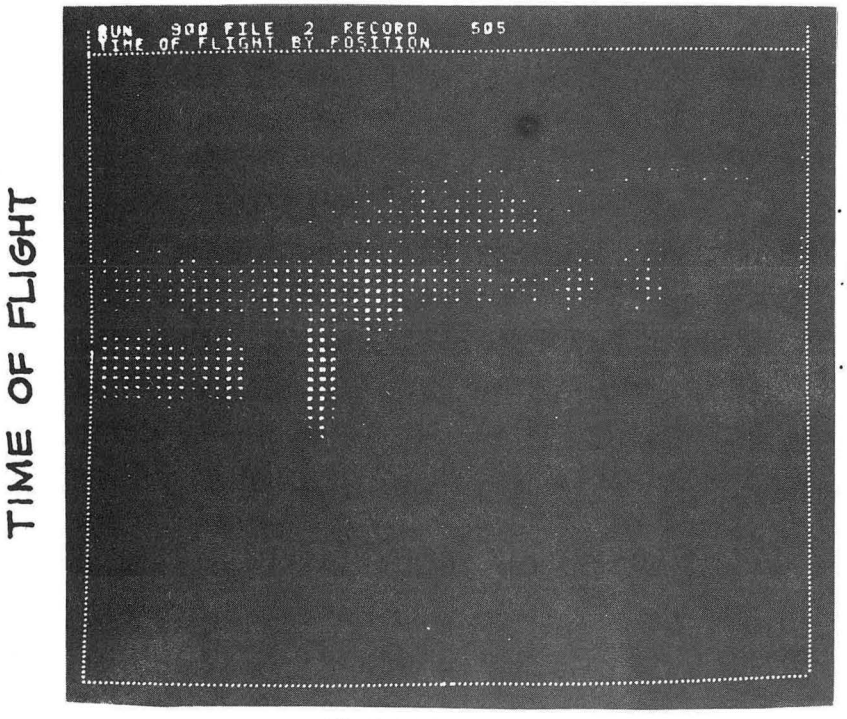

XBB 724-2196

Fig. 11

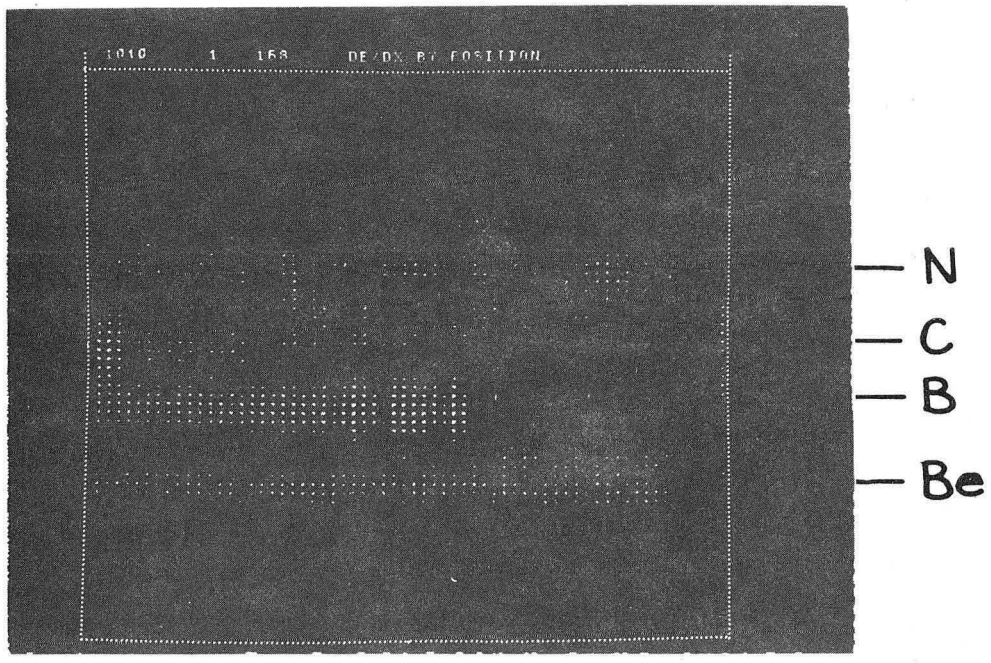

XBB 724-2197

Fig. 12

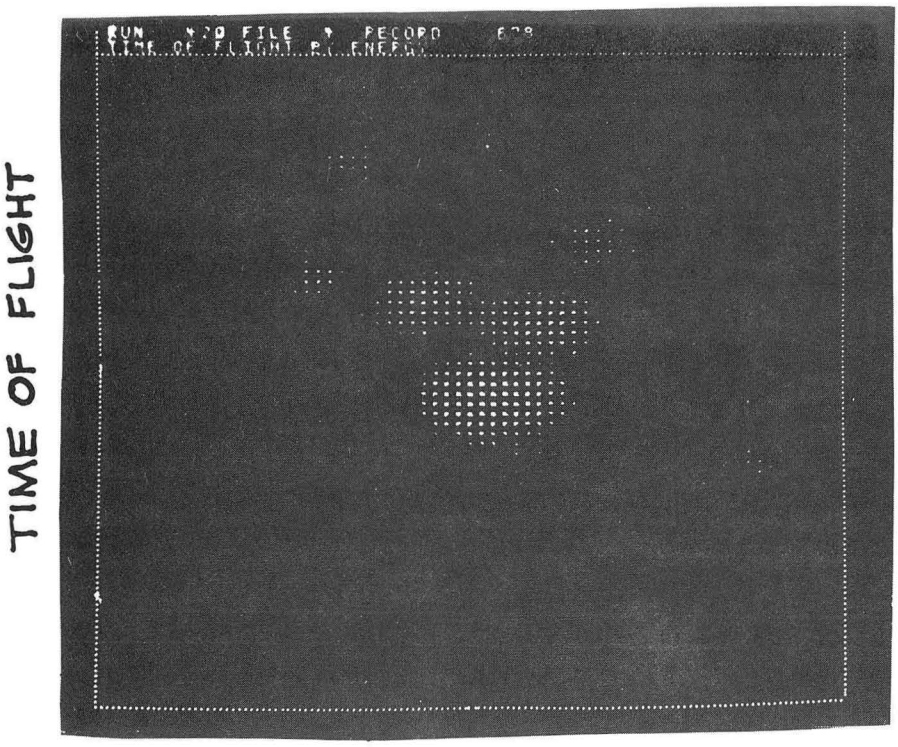

XBB 724-2195

Fig. 13

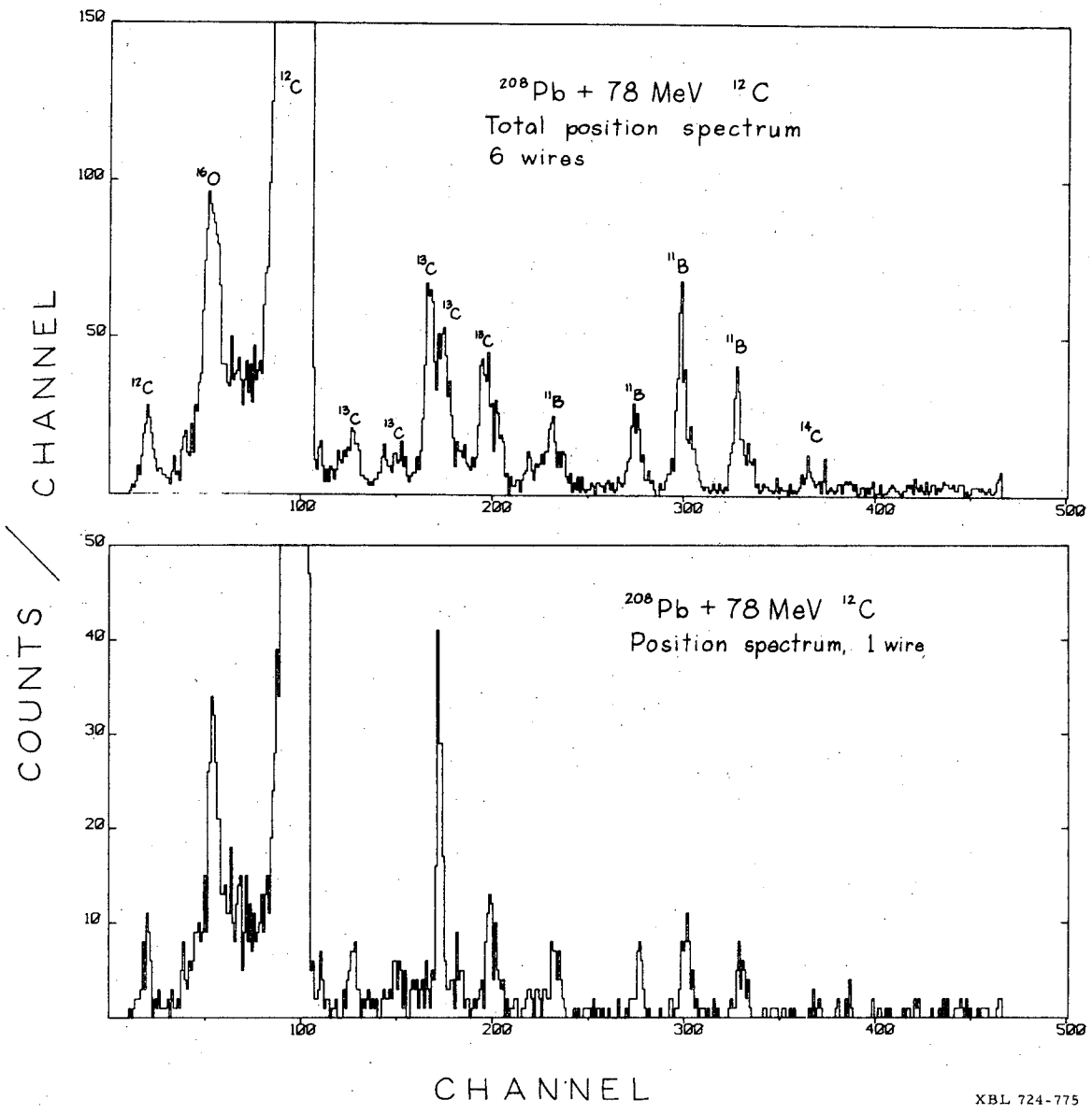
208Pb + 78 MeV 12C
Total position spectrum
6 wires
208Pb + 78 MeV 12C
Position spectrum, 1 wire
CHANNEL
COUNTS
CHANNEL
XBL 724-775

Fig. 14

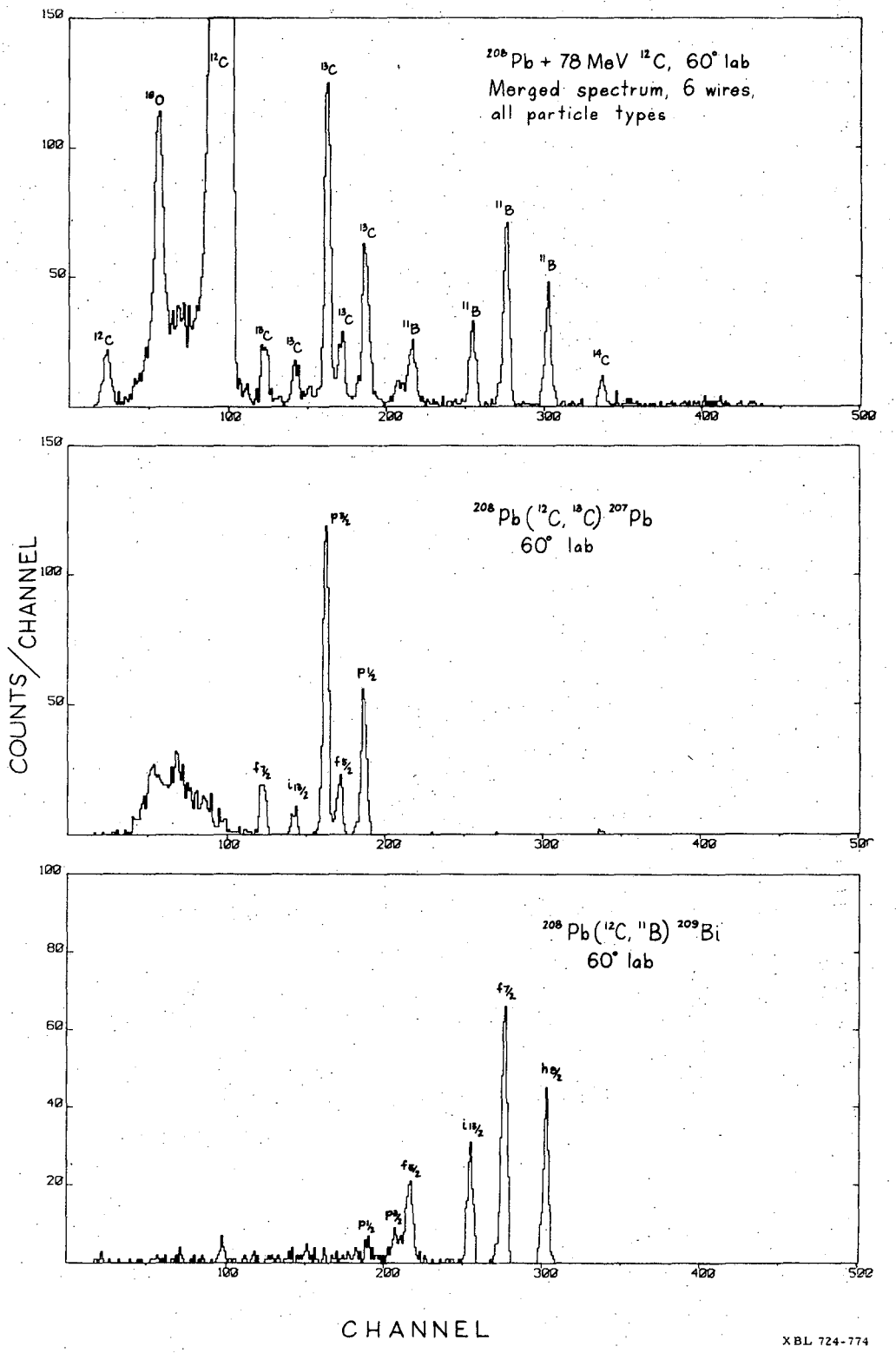
208Pb + 78 MeV 12C, 60° lab
Merged spectrum, 6 wires, all particle types
208Pb(12C, 13C)207Pb
60° lab
208Pb(12C, 11B)209Bi
60° lab
COUNTS/CHANNEL
CHANNEL
XBL 724-774

Fig. 15

TECHNICAL INFORMATION DIVISION
LAWRENCE BERKELEY LABORATORY
UNIVERSITY OF CALIFORNIA
BERKELEY, CALIFORNIA 94720